Current Chemistry Letters 15 (2026) 147–160

Contents lists available at GrowingScience

Current Chemistry Letters

homepage: www.GrowingScience.com

Theoretical design and optoelectronic properties of novel donor–acceptor–donor thieno[3,4-b]pyrazine derivatives for organic solar cells

Mustapha Elhadjaoui[a], Ahmed Azaid[a], Mohamed Ouabane[a], Morad Chemek[b,c] and Mohammed Bouachrine[a*]

[a]*Laboratory of Molecular Chemistry and Natural Substances, Moulay Ismail University, 50000 Meknes, Morocco*
[b]*Research Laboratory: Asymmetric Synthesis and Molecular Engineering of Organic Materials for Organic Electronics (LR18ES19), Faculty of Sciences, University of Monastir, 5000 Monastir, Tunisia*
[c]*Higher Institute of Applied Sciences and Technology of Sousse, University of Sousse, 4000 Sousse, Tunisia*

C H R O N I C L E

Article history:
Received April 10, 2025
Received in revised form
June 12, 2025
Accepted October 2, 2025
Available online
October 2, 2025

Keywords:
Organic solar cells
π-Conjugated systems
Thieno[3,4-b]pyrazine
BHJ

A B S T R A C T

Due to the increasing scarcity of fossil fuels and the growing demand for energy, it has become necessary to research new renewable energy sources for high-performance organic photovoltaic materials. In this context, a series of new donor–acceptor–donor compounds, based on the thieno[3,4-b]pyrazine core unit, have been designed and theoretically investigated. Donor moieties were introduced to design novel derivatives aimed at enhancing both optical absorption and charge transport properties, denoted respectively as: PTH, PTH4PF, PTH4POME, and PTHCBZ. The geometric, electronic, optical and photovoltaic characteristics of these molecular structures have been studied in depth through extensive theoretical studies. Exhibited energy gap ($E_{H\text{-}L}$ =E_{HOMO} - E_{LUMO}) ranging from 2.48 to 2.32 eV, with absorption wavelengths (λ_{abs}) between 552 and 589 nm. The V_{oc} obtained values ranged from 0.77 to 0.99 V, while the LHE values varied between 0.59 and 0.87. This study highlights the impact of structural modifications on the electronic and photovoltaic properties of organic molecules, providing valuable guidance for the experimental design of high-efficiency organic solar cells.

© 2026 by the authors; licensee Growing Science, Canada.

1. Introduction

Throughout the past century, energy sources have been at the heart origin of the development and progress of human societies, including biomass[1] and fossil hydrocarbons, which are widely used across all sectors and aspects of daily life[2] Nonetheless, the overexploitation of these non-renewable sources has caused a number of serious environmental problems, such as air and water pollution[3] global warming[4], depletion of the ozone layer[5], and the rising of sea level[6]. In this context, it has become a major challenge nowadays to replace energy generated from fossil fuels with renewable and clean energy. Wind energy[7], hydro energy[8], biomass[9], and solar energy[10,11] are among the alternatives that have been extensively researched. Among the up-and-coming technologies, solar energy benefits from organic photovoltaics (OPV) in a growing, very dynamic field[12], which has the potential to meet the increasing demand for lightweight, flexible, low-cost, and environmentally friendly devices[13,15]. Organic devices, especially organic solar cells (OSCs)[16,18], organic light emitting diodes (OLEDs)[19] and organic field effect transistors (OFETs)[20], can be used in various applications[21,22]. Currently, research is focusing on creating new organic materials that combine donor and acceptor units with π-bridges, aiming for low band-gap systems while exploring how molecular structure affects photovoltaic properties[23, 25]. Among the heterocyclic molecules studied are 2-substituted benzothiazoles, thiazolo[4,5-b]pyridines, thieno[3,4-b]pyrazines, and thiophene derivatives. Five-membered sulfur-containing heterocycles, in particular, are of great interest in modern chemistry because of their unique electronic properties, chemical stability, and versatility. They are widely used as building blocks in optoelectronic materials, helping to improve charge transport, tune the HOMO–LUMO gap, and enhance light absorption. Recent reviews emphasize their key role in developing high-performance organic semiconductors and photovoltaic devices[26, 29].

* Corresponding author
E-mail address m.bouachrine@umi.ac.ma (M. Bouachrine)
© 2026 by the authors; licensee Growing Science, Canada
doi: 10.5267/j.ccl.2025.10.003

The thieno[3,4-b]pyrazines have been extensively studied as the component of functional materials[30]. The acceptors in such monomers provide longer π-conjugated systems and lower bandgap when inserted into D-A-D type compounds that are flanked with electron-rich donor units[31]. Here, with the help of a recently synthesized D-A-D molecule by N. Cheminet et al.[32], we are setting our eyes on a D-A-D molecule having as structure-linkage bridge connecting scraps of its donor and acceptor that are composed of thiophene and thieno[3,4-b]pyrazine groups. To enhance their light and electronic properties in solar cells, we changed the donor design of the original molecule to create four new versions: PTH, PTH4PF, PTH4POME, and PTHCBZ. We are conducting a thorough theoretical study of the geometric structures and optoelectronic properties of these derivatives, including the energy gap, open circuit voltage (V_{oc}), and optical nonlinearity (ONL). This comparative study is targeted to discover and establish molecular structures with an optimized performance that could be incorporated in future organic solar cells.

2. Preparation of Thieno[3,4-b]pyrazines

Thieno[3,4-b]pyrazines are recognized compounds in a group of organic compounds that have a specific arrangement of thiophene, and pyrazine rings close together in the same plane[33]. These oligomers have garnered considerable research interest for organic electronic materials[31] due to their distinctive structure, excellent electronic and optical properties, and low bandgap, which are considered promising for organic solar cells, organic field-effect transistors (OFETs), and organic light-emitting diodes (OLEDs)[34]. The most common way to make thieno[3,4-b]pyrazines involve reacting 3,4-diaminothiophene with a 1,2-diketone. In this route, 3,4-diaminothiophene is produced in situ from an ammonium salt in the presence of triethylamine as a blocking base[32] according to the synthetic scheme such as shown in **Fig. 1**.

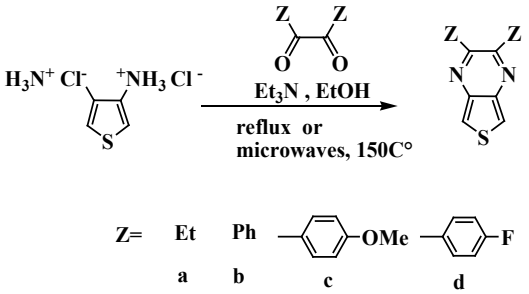

Fig. 1. Synthesis of thienopyrazine derivatives a-d[32]

To explore the diversity of the substituent Z, two methods of condensation with an excess of 1,2-diketone were investigated. Only four of them were separated by flash chromatography (a, b, c and d). DFT calculations found out that incorporating pyrazine to thiophene can remarkably lower the LUMO energy level, decrease the energy gap (E_g), and prolong the conjugation. The effect of the substituent Z on energy levels is shown through ultraviolet photoelectrons spectroscopy experiments (UPS) and optical absorption experiments, which reveal how the electronic and optical properties of thienopyrazines can be adjusted.

We have summarized in (**Table 1**) the optoélectronique and absorption proprieties of the synthesized compounds a, b, c, and d. these properties, determined in $CHCl_3$ solution, include the values of E_{gap}, E_{HOMO}, and E_{LUMO}, obtained from DFT and TD-DFT calculations according to reference [32]. From this table, we can see that the maximum experimental absorption wavelengths (λ_{max} in $CHCl_3$) vary between 315 and 378 nm, while the values calculated by TD-DFT range from 281 to 398 nm. Although there are some discrepancies, the general trends remain consistent: both sets of data show a red shift in the absorption maxima as a function of structural changes in the molecules. Similarly, the optical gaps obtained from the experimental UV–Vis spectra range from 3.11 to 4.40 eV, while the calculated HOMO–LUMO gaps vary from 3.13 to 4.05 eV. The differences, generally between 0.3 and 0.4 eV, are acceptable given the approximations inherent in DFT methods. This correlation confirms the relevance of the computational methodology used.

Table 1. Electronic properties of compounds a-d[32]

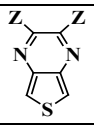

Z	Compound	yield a : method 1 b : method 2	λ_{max} Absorption (nm) ($CHCl_3$)	λ_{max} Absorption (nm) (TD-DFT)	Optical-Gap (eV) (DFT)	$\Delta E = (E_{LUMO} - E_{HOMO})$ (eV)
Et	a	51 %a	315	281	4.40	4.05
Ph	b	26 %a 20 %b	347	357	3.46	3.75
Ph-OMe	c	22 %a	378	398	3.11	3.72
Ph-F	d	43 %a 30 %b	348	366	3.38	3.13

3. Methodology and DFT calculations

Quantum chemistry calculations facilitate the prediction and design of new organic materials for optoelectronic applications[35,36]. In this work, quantum chemical calculations were performed to investigate the electronic properties of the studied molecules using density functional theory (DFT)[37]. The B3LYP functional, combined with the 6-31G(d,p) basis set, was used to optimize the molecular geometries, resulting in stable structures[28, 38]. The B3LYP hybrid functional was employed for geometry optimizations because it has long been recognized for providing a reliable balance between accuracy and computational cost in predicting ground-state structures of π-conjugated organic systems, which are central to photovoltaic applications. Although B3LYP can sometimes underestimate the energy gaps for highly conjugated molecules, its consistent performance in reproducing experi mental geometries and electronic distributions makes it a widely accepted choice in organic electronics research[39, 43].

This method guarantees the minimization of the total energy of the system, giving an optimum description of the compounds' structures[44]. In order to elucidate the optical properties of the studied compounds, TD-DFT approach was employed with the B3LYP functional and the 6-31G(d,p) basis set. The electronic absorption spectra and the calculated maximum absorption (λ_{max}) and the optical band gap were elucidated, we studied how electrons migrate between the excited and ground states, and we obtained a detailed explanation of the absorption spectra. All simulations were performed using Gaussian 09 program, which is widely employed for quantum chemical investigations. To understand and analyze the molecular orbitals, GaussView 6.0 was employed, which represented them clearly and in detail. ChemDraw Ultra 7.0[45] was used to draw molecular structures and generate 2D models for the compounds (**Fig. 2**).

UV-vis absorption spectra and density of states (DOS) spectra were created using Origin 7.0, a software that helps analyze and display both experimental and complex theoretical data by calculating absorption profiles and the electronic states in the compounds.

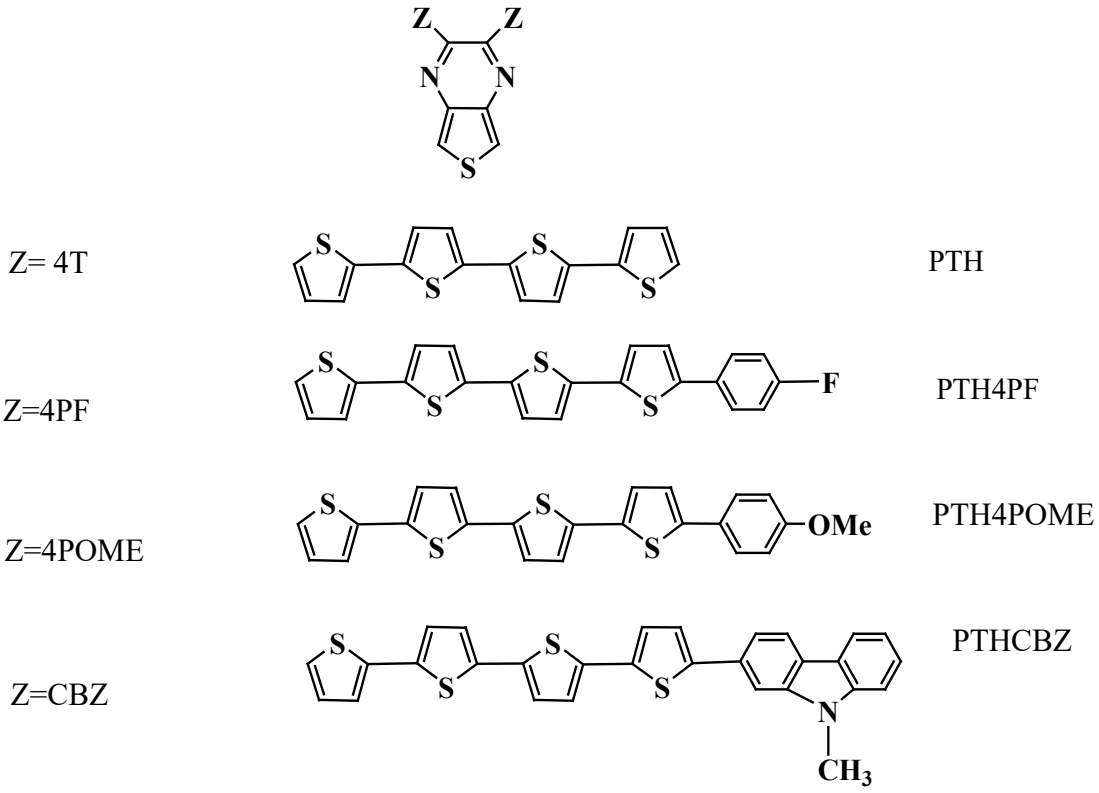

Fig. 2. Structure of studied molecules

4. Results and discussion

4.1. Geometrical properties

The study of bond lengths and dihedral angles is essential to understanding molecular structure and its electronic properties. These parameters influence electronic conjugation and the planarity of the system, directly affecting charge mobility and the optical behavior of the molecules[31]. Indeed, the bond lengths (d_i in Å) do not increase over the set of the studied molecules and are quite close to one another, going from 1.44 Å to 1.46 Å (**Table 2**). These values constitute proof of very good conjugation over the π-system, evidence of a very efficient electronic delocalization from donor to acceptor

(**Fig. 3**). These consistent bond lengths agree quite well with the strong conjugated system, which is important for its electronic properties, including charge transport and optical behavior.

Beyond bond lengths, the dihedral angles (θ_i) provide important information on the planarity of the molecular structures. For all molecules, dihedral angles fall between 152° and 170° (**Table 3**) and therefore seem to be almost planar, albeit with some small twisting relaxations. This slight bending is typical in organic molecules with complicated conjugated systems, where the shape of some (or none) changes can be affected by steric or electronic distortions[47,48]. The distortions with the substituents in PTH4PF, PTH4POME, and PTHCBZ compounds are low when compared to the PTH molecule itself. This evidence indicates that the geometry is not extensively distorted upon functionalization of the system. It is noteworthy that the dihedral angle θ_5(°) of the end group is also larger than 150°, indicating the maintenance of planarity even after modification. Maintaining a planar structure is quite beneficial as far as π-conjugation, charge transfer, and charge mobility are concerned, which are ideal properties for optoelectronic applications. Indeed, the results obtained for the dihedral angles and bond lengths of the different studied molecules show that the modifications made do not cause significant distortions to the molecular structure. This preservation of planarity promotes efficient delocalization of the π electrons, which is crucial for the molecules' electronic and optical properties. The dihedral angles θ_i (i = 1–5) and bond lengths di (i = 1–5) of the molecules PTH, PTH4PF, PTH4FOM, and PTHCBZ are shown in the following Tables.

Table 2. Bond lengths of the molecules studied

Studied molecules	d_1(Å)	d_2(Å)	d_3(Å)	d_4(Å)	d_5(Å)
PTH	1.46	1.44	1.44	1.44	-
PTH4PF	1.46	1.44	1.44	1.44	1.46
PTH4POME	1.46	1.44	1.44	1.44	1.46
PTHCBZ	1.46	1.44	1.44	1.44	1.46

Table 3. Dihedral angles of the studied compounds

Studied Molecules	θ_1(°)	θ_2(°)	θ_3(°)	θ_4(°)	θ_5(°)
PTH	160.54	-167.95	-164.93	-163.28	-
PTH4PF	160.46	-168.40	165.48	-165.18	153.02
PTH4POME	160.45	-168.60	166.19	-165.96	154.04
PTHCBZ	160.42	-167.81	167.19	-170.72	-152.10

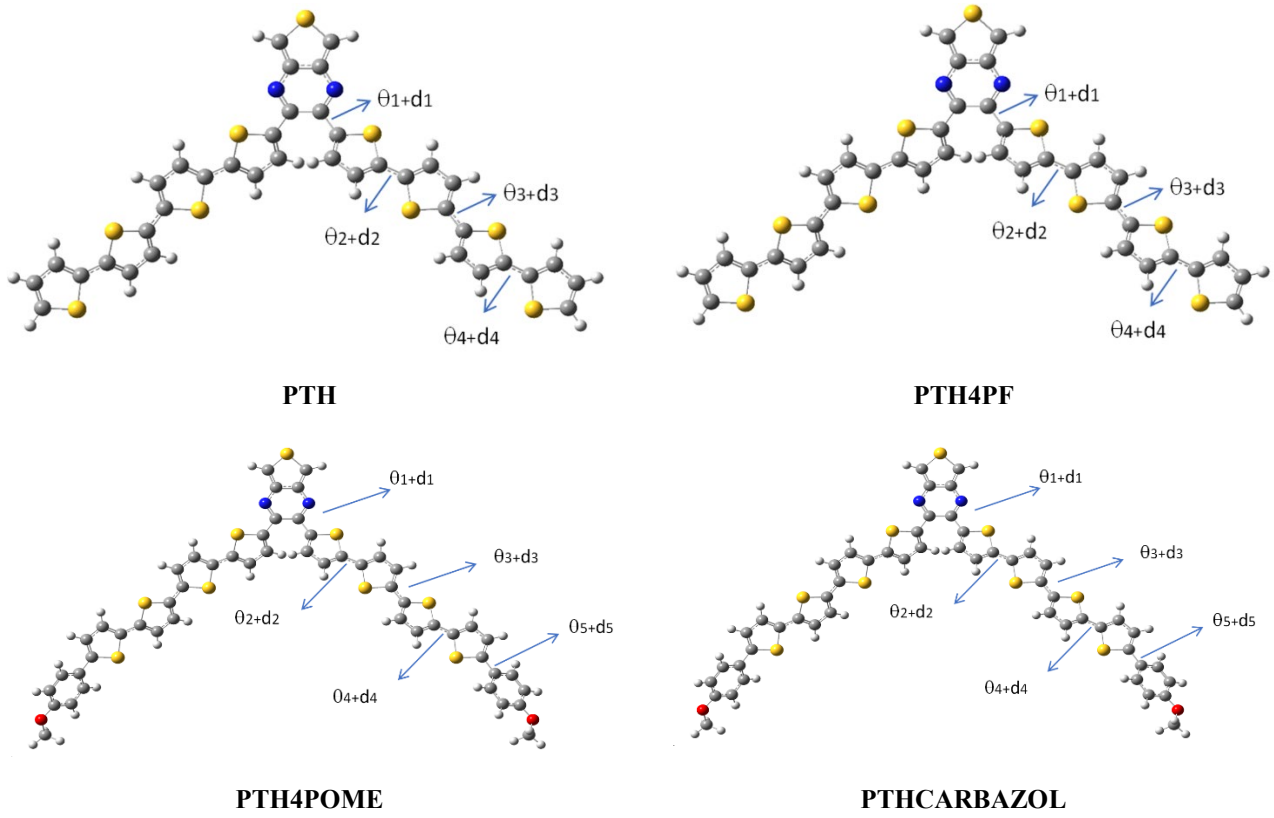

Fig. 3. the optimized structure of the molecules studied

4.2. Quantum chemical properties

4.2.1. optoelectronic properties and Density of States (DOS)

The energy of the highest occupied molecular orbital (E_{HOMO}) and the energy of the lowest unoccupied molecular orbital (E_{LUMO}) of the studied molecules were examined using DFT calculations at the B3LYP/6-31G(d,p) level[49] The separation of these two levels, termed the energy gap (E_{gap}). The efficiency of organic solar cell (OSC) devices is strongly related to their energy gap (E_{gap}). A lower energy gap generally leads to enhanced charge transfer capability and a higher maximum absorption wavelength (λ_{max})[50]. As shown in **Table 4**, the theoretical value of the energy of the HOMO level for the molecules studied is -4.99, -4.97, -4.83 and -4.77 eV respectively for the molecules PTH, PTH4PF, PTH4OME and PTHCBZ. The energies of the corresponding LUMO orbitals are: -2.51; -2.54; -2.46 and -2.44 eV. In addition, energy gap $E_{H-L}=E_{HOMO}-E_{LUMO}$ decreases in the following order: E_{H-L} (PTH)> E_{H-L} (PTH4PF)> E_{H-L} (PTH4POME) > E_{H-L} (PTHCBZ). These results show that all the molecules studied have a low energy gap, between 2.48 eV and 2.32 eV, while the energy gap values of the base molecule are between 4.05 eV and 3.38 eV (**Table 1**). This indicates efficient light absorption and charge transfer. Density of states (DOS) analysis plays an interesting role in determining the charge distribution in the molecules studied[51]. To confirm the previous results a density of states analysis was performed using the B3LYP/6-31G(d,p) method, and the results are shown in **Fig. 5**. The DOS analysis shows that HOMO states are predominantly located on electron donor nuclei, while LUMO states are focused on acceptor groups. These DOS profiles confirm an efficient charge transfer from donor to acceptor. In summary, the results show that structural modification of the basic molecule generates new molecules that could be good candidates for improving the performance of organic solar cells (OSCs).

Table 4. E_{HOMO} (eV), E_{LUMO} (eV) and E_{H-L} (eV) of the studied molecules

Studied molecules	E_{HOMO} (eV)	E_{LUMO} (eV)	E_{H-L} (eV)
PTH	-4.99	-2.51	2.48
PTH4PF	-4.97	-2.54	2.42
PTH4POME	-4.83	-2.46	2.36
PTHCBZ	-4.77	-2.44	2.32

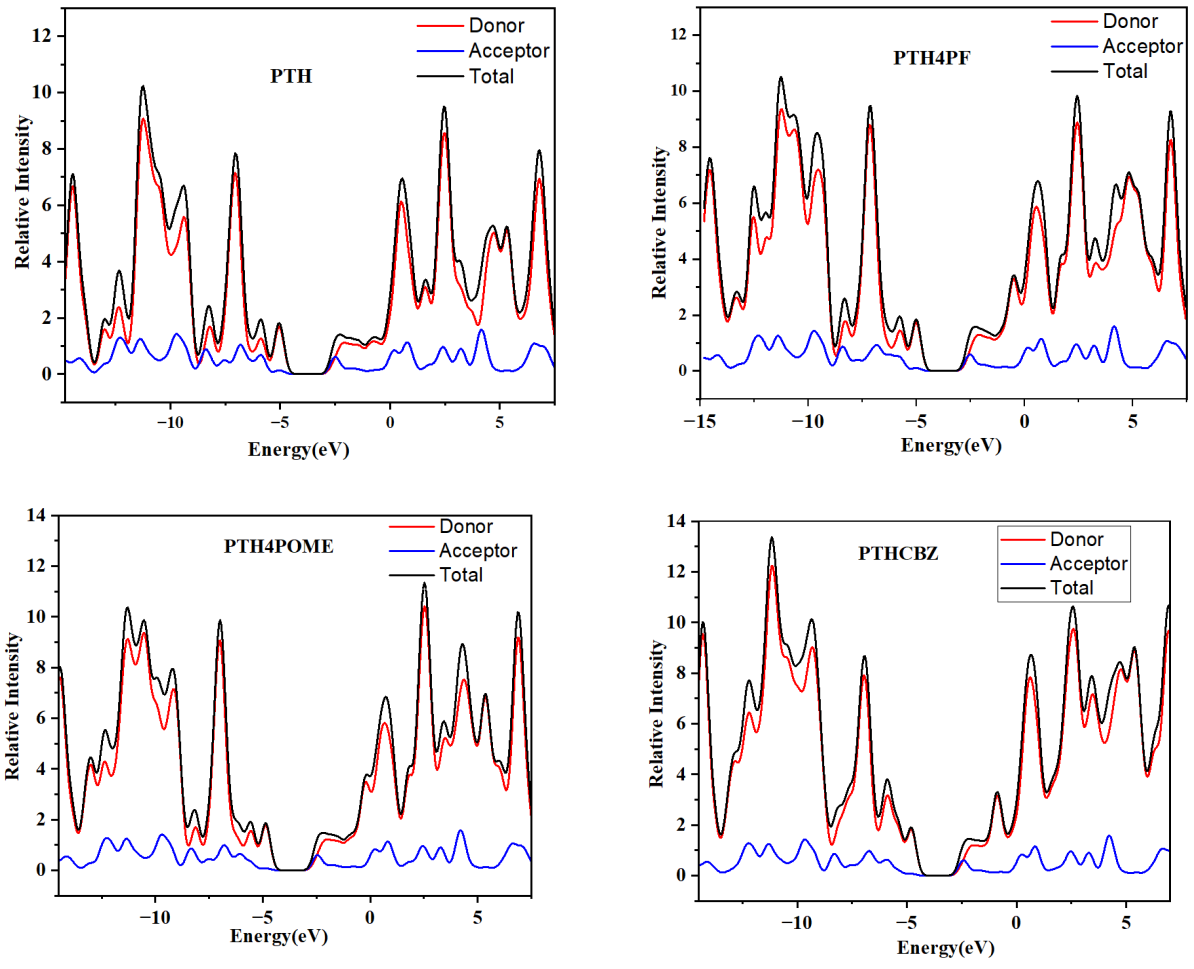

Fig. 5. Density of States diagram of the four molecules (DOS)

4.2.2. Chemical Reactivity Index

The HOMO and LUMO energy levels play a fundamental role in determining the reactivity of molecules. In particular, they make it possible to estimate important quantities such as the chemical potential (μ), electronegativity (χ) and overall chemical hardness (η)[52]. These parameters can be calculated using equations (1), (2) and (3), and the values obtained are presented in **Table 5**. Chemical potential (μ), the opposite of which corresponds to electronegativity, reflects the tendency of a system to attract electrons. A negative chemical potential for a stable system indicates that it does not spontaneously dissociate into its elementary constituents[53]. Chemical hardness (η) expresses the resistance of a system to the perturbation of its electron cloud. It represents the system's ability to resist electronic variations induced by a chemical process[54]. As shown in **Table 5**, the chemical potential values (μ) of the four molecules follow the following ascending order: PTH4PF (-3.76 eV) < PTH (-3.75 eV) < PTH4POME (-3.64 eV) < PTHCBZ (-3.60 eV). In terms of chemical hardness (η), the PTHCBZ molecule has the lowest value, with respective hardnesses of 1.21 eV, 1.24 eV, 1.18 eV and 1.16 eV for PTH4PF, PTH, PTH4POME and PTHCBZ.

$$\mu = (E_{LUMO} + E_{HOMO})/2 \quad (1)$$
$$\eta = (E_{LUMO} - E_{HOMO})/2 \quad (2)$$
$$\chi = -(E_{LUMO} + E_{HOMO})/2 \quad (3)$$

Table 5. Chemical reactivity indices (in eV) for the four compounds

Studied molecules	μ (eV)	η (eV)	χ (eV)
PTH	-3.75	1.24	3.75
PTH4PF	-3.76	1.21	3.76
PTH4POME	-3.64	1.18	3.64
PTHCBZ	-3.60	1.16	3.60

4.2.3. Molecular Electrostatic Potential Surface (MEP)

Molecular Electrostatic Potential (MEP) analysis provides crucial insights into the electronic distribution of organic molecules, allowing for the identification of regions susceptible to nucleophilic and electrophilic attacks, as well as potential sites for intermolecular interactions such as hydrogen bonding[55-57]. The MEP maps of the investigated compounds, calculated at the B3LYP/6-31G(d,p) level of theory, are depicted in **Fig. 6**.

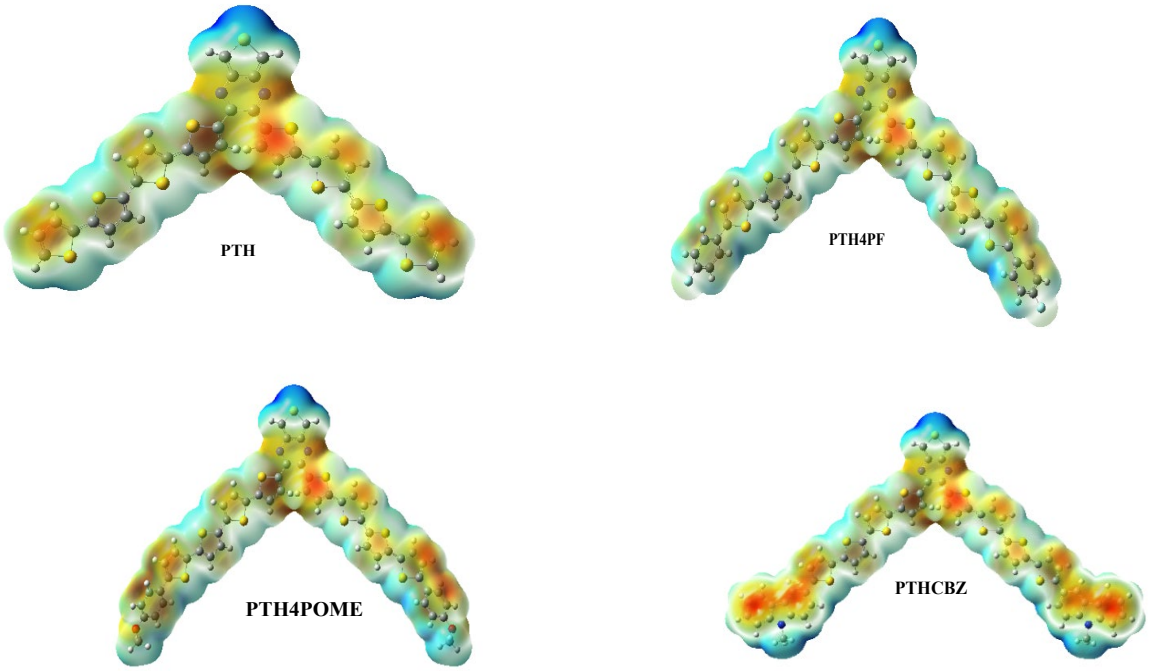

Fig. 6. MEP maps of the studied molecules

The Molecular Electrostatic Potential (MEP) map reveals regions of varying electrostatic potential. Areas in red indicate negative potential, corresponding to nucleophilic sites. Conversely, blue regions represent positive potential, identifying

electrophilic sites. Green areas are considered electrostatically neutral. The potential gradually increases in the color sequence: red < orange < yellow < green < blue[58]. As shown in **Fig. 6**, the MEP analysis reveals that the positive region (blue area) is mainly located on the thiophene moiety as well as on two fluorine atoms attached to the thiophene system. The PTH4PF and PTHCBZ molecules show a blue zone around the hydrogen atoms linked to the methoxy and carbazole units respectively, indicating an electropositive region. On the other hand, an increase in the negative region (red zone) is observed around the donor groups in all the molecules, reflecting a higher electron density in these zones.

4.3. Optical properties

Based on the optimized chemical structure of the modified thienopyrazine, the simulated optical absorption spectra of the studied molecules are obtained using TD-DFT/B3LYP/6-31G(d,p) level of theory. The simulated optical absorption spectra of the modified thienopyrazine are depicted in **Fig. 7**.

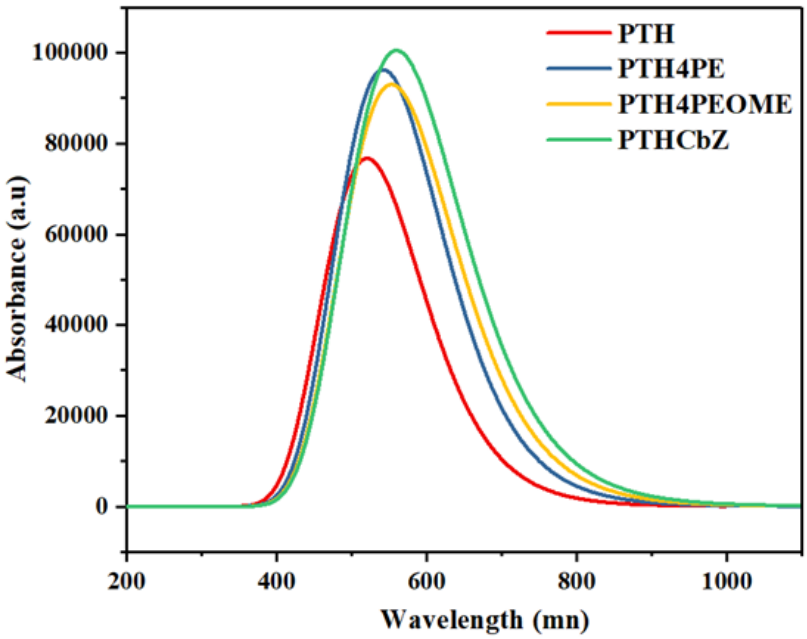

Fig. 7. Absorption spectra of the studied molecules

In contrast with the unmodified thienopyrazine, the modified molecules present a large absorption in the visible-near infrared region, suggesting the obtain of good newly materials for photovoltaic application. Based on the obtained simulated optical absorption spectra various parameters such as λ_{max}, vertical excitation energies (E_{ex}), oscillator strengths (f), major transitions (MO) and % contribution, are obtained and presented in **Table 6**.

Table 6. Absorption maxima (λ_{max}), excitation energies (E_{ex}), oscillator strengths (f), light harvesting efficiency (LHE), and probable transitions

Compounds	λ_{max} (nm)	E_{ex} (eV)	f	LHE	MO/Character
PTH	552.43	2.24	0.38	0.59	HOMO→ LUMO (97%)
	544.38	2.27	0.57		HOMO-1→ LUMO (99%)
	498.66	2.48	1.07		HOMO→ LUMO+1 (97%)
PTH4PF	564.79	2.19	0.49	0.67	HOMO→ LUMO (98%)
	561.62	2.20	0.90		HOMO-1→ LUMO (96%)
	517.52	2.39	1.11		HOMO→ LUMO+1(93%)
PTH4POME	579.33	2.14	0.48	0.66	HOMO→ LUMO (98%)
	579.30	2.14	0.83		HOMO-1→ LUMO (96%)
	524.93	2.36	1.15		HOMO→ LUMO+1 (94%)
PTHCBZ	589.33	2.10	0.92	0.87	HOMO-1→ LUMO (94%)
	587.32	2.11	0.49		HOMO→ LUMO (97%)
	530.18	2.33	1.28		HOMO→ LUMO+1 (93%)

The theoretical λ_{max} of the unmodified molecule varies from 281 nm to 366 nm[32], whereas the modified molecules depict the λ_{max} values from 552.43 nm to 589.33 nm. This displacement is related to the influence of the substituents on the absorption wavelength and optical bandgap. A redshift is observed from the PTH molecule (552.43 nm) to the PTHCBZ molecule (589.33 nm). This phenomenon is accompanied by a decrease in the excitation energy (E_{ex}), which reflects a reduction in the optical bandgap (E_g). The oscillator strength (f) values indicate that PTHCBZ absorbs more solar light in

the visible range (f = 1.28 at 530.18 nm), meaning it can capture sunlight better over a wider area, which is a good sign for organic solar cells (OSCs). The λ_{max} values for all the compounds are as follows: PTH < PTH4PF < PTH4POME < PTHCBZ. The excitation energies for the compounds (PTH, PTH4PF, PTH4POME, and PTHCBZ) are 2.24 eV, 2.19 eV, 2.14 eV, and 2.10 eV, respectively. Additionally, the oscillator strengths (f) for these compounds are 0.38, 0.49, 0.48, and 0.92, respectively. It should be noted that the oscillator strength (f) is related to the maximum absorption wavelength and provides information about light harvesting efficiency (LHF) by the following relation[59]:

$$LHE = 1 - 10^{-f} \quad (4)$$

The (LHE) is a key parameter for organic solar cells (OSC). A high LHE indicates a greater capacity of the materials to absorb the majority of photons in the UV-visible region[60]. The LHE values measured for the compounds studied follow this order: PTH (0.59 eV) < PTH4PF (0.67 eV) < PTH4POME (0.66 eV) < PTHCBZ (0.87 eV).

4.4. Photovoltaic Properties

The properties of photovoltaic devices are primarily determined by electrons transitioning from the valence band to the conduction band, in terms of fullerene derivatives[61]. For effective exciton dissociation, the lowest unoccupied molecular orbital energy (E_{LUMO}) of the donor must be at least 0.3 eV higher than the E_{LUMO} of the acceptor[62]. The value of α is the difference between the E_{LUMO} energy levels of the molecules under study and the acceptor, which is determined by equation (5)[63]. This research concerns on electronic properties of materials in a DSSC and show the influence of the energy level differences for the charge separation process, which will make the contribution to increase the performance of the light-to-electricity conversion efficiency.

$$\alpha = E_{LUMO}(Donor) - E_{HOMO}(Acceptor) \quad (5)$$

The open-circuit voltage (V_{oc}) is one of the important parameters that determine the performance of organic solar cells. V_{oc} is the highest potential a device can achieve in an open-circuit state in Bulk Heterojunction (BHJ). This voltage is determined by the offset between the energy levels of the HOMO of the donor and the LUMO of the acceptor, considering the energy loss during the generation of photogenerated charges[62-64]. Where, V_{oc} is estimated from the equation (6), this expression takes into account the difference in energy levels between the donor and acceptor frontier orbitals, as well as an empirical energy loss of 0.3 eV related to real phenomena in the organic solar cell[65] as:

$$V_{oc} = \frac{1}{e}\left(|E_{HOMO}(Donor)| - |E_{LUMO}(Acceptor)\right) - 0.3 \quad (6)$$

Table 7 shows the energy levels including E_{HOMO}, E_{LUMO}, V_{oc}, and the α values. For the determination of the V_{oc}, $PC_{61}BM$ was selected as the acceptor because of its relatively high energy levels (0.3 – 0.67 V) and due to its wide distribution and use in the literature when compared to other acceptors[66]. Analysis of these results reveals that the best donor, as quantified by the value of the V_{oc}, is PTH (0.998 V), followed by PTH4PF (0.975 V), PTH4POME (0.830 V), and lastly PTHCBZ (0.77 V).

Table 7. The Photovoltaic parameters E_{HOMO}, E_{LUMO}, V_{oc}, and the α values of the studied compounds

Studied molecules	E_{HOMO} (eV)	E_{LUMO} (eV)	V_{OC} (V)	α
PTH	-4.99	-2.51	0.99	1.18
PTH4PF	-4.97	-2.54	0.97	1.15
PTH4POME	-4.83	-2.46	0.83	1.23
PTHCBZ	-4.77	-2.44	0.77	1.25
$PC_{61}BM$	-6.10	-3.70	-	-

The investigation of the photovoltaic properties of the studied compounds indicates an energetically favorable alignment for efficient exciton dissociation, as evidenced by α values exceeding the threshold of 0.3 eV. Moreover, the calculated open-circuit voltages (V_{oc}) demonstrate suitable electronic compatibility for the effective integration of these donor materials into bulk heterojunction (BHJ) organic solar cells.

4.5. Nonlinear optical properties (NLO)

The nonlinear optical (NLO) properties of materials, resulting from their interaction with high intensity electromagnetic fields, play a fundamental role in many advanced technological applications, such as optical switches, optical information processing, optical data storage devices and optical communication technologies[67]. These properties are closely related to the electronic structure of the compounds, particularly their ability to facilitate intramolecular charge delocalization[68]. Efficient delocalization of electron density significantly enhances the nonlinear optical response, which is commonly

characterized by key parameters such as the average polarizability (α) and the first-order hyperpolarizability (β)[69]. These quantities can be calculated using quantum computational methods, including density functional theory (DFT). Indeed, analyzing nonlinear optical properties is a powerful approach to evaluating charge transfer dynamics in organic materials. This method provides valuable insights into photovoltaic performance, especially regarding critical parameters such as the short-circuit current density (J_{SC}) and the power conversion efficiency. The polarizability (α) and hyperpolarizability (β) values can be determined following Eq. (7) and Eq. (8)[70] and the properties obtained for these compounds are presented in **Table 8**.

Analysis of the results presented in **Table 8** reveals that the molecular polarizability (α) of the compounds studied follows an ascending order defined as follows: α(PTH) = 135 esu < α(PTH4PF) = 173.942 esu < α(PTH4POME) = 184.412 esu < α(PTHCBZ) = 215.363 esu. The PTHCBZ molecule thus has the highest polarizability value. Furthermore, the first values of hyperpolarizability (β) of the same molecules are ordered in an increasing manner as follows: β(PTH) = 248.687 esu < β(PTH4PF) = 330.842 esu < β(PTH4POME) = 532.404 esu < β(PTHCBZ) = 691.911 esu. It can be seen that for the NLO studies, the values of non-linear optical response of all compounds studied are higher than that of urea[71, 72]. It is also worth noticing that the β factors converge for decreasing energy gaps. Large NLO coefficients mean that the D-π-A molecule can efficiently transfer the charge from the donor group to the acceptor group in the molecular.

$$\alpha = \frac{1}{3}(\alpha_{xx}+\alpha_{yy}+\alpha_{zz}) \tag{7}$$

$$\beta = \sqrt{\beta_x{}^2 + \beta_y{}^2 + \beta_z{}^2} \tag{8}$$

xx, yy, zz represent the tensorial coefficients of the polarizability, and β_i = (i = x, y, z) combines the different quantities:

$$\beta_i = \left(\frac{1}{3}\right)\sum_{i=x,y,z}(\beta_{ijj} + \beta_{jij} + \beta_{jji}) \tag{9}$$

Table 8. Polarizability (α) and hyperpolarizability (β) and the corresponding tensor components

Parameters	PTH	PTH4PF	PTH4POME	PTHCBZ
α_{xx}	201.000	254.364	265.119	337.232
α_{xy}	0.000	0.000	0.004	-0.222
α_{yy}	166.000	218.054	235.280	256.806
α_{xz}	-11.900	-16.356	-15.798	-7.001
α_{yz}	0.000	0.000	0.001	-0.595
α_{zz}	37.500	49.409	52.836	52.052
α [10^{-24}esu]	135.000	173.942	184.412	215.363
β_{xxx}	-0.005	0.000	-0.020	0.660
β_{xxy}	-139.377	-190.917	-309.366	-429.352
β_{xyy}	-0.001	0.000	-0.014	0.362
β_{yyy}	-109.609	-140.694	-224.304	-263.183
β_{xxz}	-0.002	0.000	0.001	-0.423
β_{xyz}	-5.593	-7.018	-5.358	-2.860
β_{yyz}	-0.001	0.000	0.000	-0.129
β_{xzz}	0.000	0.000	0.000	0.000
β_{yzz}	0.300	0.769	1.267	0.625
β_{zzz}	0.000	0.000	0.000	0.248
β [10^{-30}esu]	248.687	330.842	532.404	691.911

5. Conclusion

This theoretical study, based on DFT and TD-DFT methods, investigated four compounds derived from a thiophenopyazine-based molecule aiming to enhance their electronic, optical, and photovoltaic properties.

Structural and electronic properties

Following geometric optimization, all molecules exhibited a nearly planar structure, favoring efficient π-conjugation and intramolecular charge transfer (ICT). The analyses revealed a significant reduction in the energy gap (E_{H-L}), ranging from 2.32 eV to 2.48 eV. Furthermore, these structures may be promising candidates for organic solar cells (OSCs).

Optical properties

The TD-DFT results revealed a noticeable red shift of the maximum absorption wavelengths (λ_{max}) within the visible region between 552 nm and 589 nm. These shifts, supported by the DOS plots and molecular electrostatic potential (MEP) surfaces, confirm the strong ICT character of the designed molecules and their enhanced light-harvesting ability.

Nonlinear Optic (NLO)

The nonlinear optical (NLO) properties were systematically investigated, indicating that these compounds have potential applications in nonlinear optics, The first-order hyperpolarizabilities (β_{tot}) are significantly enhanced, with values ranging from 248.687 to 691.911 × 10^{-30} esu., reinforcing their potential not only for photovoltaic applications but also for optoelectronic devices such as optical switches.

A key strength of this work is the clear correlation established between molecular design and crucial optoelectronic parameters, offering valuable predictive guidelines for the development of high-performance OSC materials. Consequently, the newly designed compounds demonstrate strong potential for advanced optoelectronic applications.

Funding

This research received no financial support.

Declaration of competing interest

The authors declare that they have no known competing financial interests or personal relationships that could have appeared to influence the work reported in this paper.

Acknowledgments

We dedicate this work to the “Moroccan Association of Theoretical Chemists” (MATC) for its pertinent help concerning the programs.

Data availability

Data will be made available on request

References

[1] Nunes L. J. R., Causer T. P., and Ciolkosz D. (**2020**) Biomass for energy: A review on supply chain management models. Renew. Sustain. Energy Rev., 120, 109658. https://doi.org/10.1016/j.rser.2019.109658.

[2] Sharif A., Baris-Tuzemen O., Uzuner G., Ozturk I., and Sinha A. (**2020**) Revisiting the role of renewable and non-renewable energy consumption on Turkey’s ecological footprint: Evidence from Quantile ARDL approach. Sustain. Cities Soc., 57, 102138. https://doi.org/10.1016/j.scs.2020.102138.

[3] Dincer I. (**1999**) Environmental impacts of energy. Energy Policy, 27, 845–854. https://doi.org/10.1016/S0301-4215(99)00068-3.

[4] Godzimirski J. M. (**2022**) Energy, climate change and security: The Russian strategic conundrum. J. Eurasian Stud., 13, 16–31. https://doi.org/10.1177/18793665211054518.

[5] Omer A. M. (**2009**) Energy use and environmental impacts: A general review. J. Renew. Sustain. Energy, 1, 053101. https://doi.org/10.1063/1.3220701.

[6] Olabi A. G., Obaideen K., Elsaid K., Wilberforce T., Sayed E. T., Maghrabie H. M., and Abdelkreem M. A. (**2022**) Assessment of the pre-combustion carbon capture contribution into sustainable development goals SDGs using novel indicators. Renew. Sustain. Energy Rev., 153, 111710. https://doi.org/10.1016/j.rser.2021.111710.

[7] Wagner H.-J. (**2018**) Introduction to wind energy systems. EPJ Web Conf., 189, 00005. https://doi.org/10.1051/epjconf/201818900005.

[8] Bilgili M., Bilirgen H., Ozbek A., Ekinci F., and Demirdelen T. (**2018**) The role of hydropower installations for sustainable energy development in Turkey and the world. Renew. Energy, 126, 755–764. https://doi.org/10.1016/j.renene.2018.03.089.

[9] Henrich E., Dahmen N., Dinjus E., and Sauer J. (**2015**) The role of biomass in a future world without fossil fuels. Chem. Ing. Tech., 87, 1667–1685. https://doi.org/10.1002/cite.201500056.

[10] Chineke T. C., and Ezike F. M. (**2010**) Political will and collaboration for electric power reform through renewable energy in Africa. Energy Policy, 38, 678–684. https://doi.org/10.1016/j.enpol.2009.10.004.

[11] Strupeit L., and Palm A. (**2016**) Overcoming barriers to renewable energy diffusion: business models for customer-sited solar photovoltaics in Japan, Germany and the United States. J. Clean Prod., 123, 124–136. https://doi.org/10.1016/j.jclepro.2015.06.120.

[12] Kacimi R., Tanıs E., Azaid A., Raftani M., Sarfaraz S., Bejjit L., and Bouachrine M. (**2023**) Benzodithiophene-based Acceptor-Donor-Acceptor-type compounds for highly efficient organic photovoltaic cells. Chem. Phys. Lett., 830, 140774. https://doi.org/10.1016/j.cplett.2023.140774.

[13] Skabara P. J. (**2013**) A brief perspective on the evolution of plastic electronics - From highly conducting polymers to conjugated organic semiconductors. Chem. Commun., 49, 9242–9244. https://doi.org/10.1039/c3cc44599b.

[14] Malik H., Niazi M. B. K., Miran W., Tawfeek A. M., Jahan Z., Kamel E. M., Ahmed N., and Akhtar M. S. (**2023**) Wood as a green and sustainable alternative for environmentally friendly & flexible electronic devices. Chemosphere, 336, 139213. https://doi.org/10.1016/j.chemosphere.2023.139213.

[15] Kacimi R., Raftani M., Abram T., Azaid A., Ziyat H., Bejjit L., Bennani M. N., and Bouachrine M. (**2021**) Theoretical design of D-π-A system new dyes candidate for DSSC application. Heliyon, 7, e07171. https://doi.org/10.1016/j.heliyon.2021.e07171.

[16] Kacimi R., Hayn R., Azaid A., Raftani M., Bejjit L., and Bouachrine M. (**2025**) Design and computational analysis of benzothiadiazole-fluorene based molecules for organic light-emitting diodes and high-efficiency organic solar cells. Mater. Sci. Semicond. Process., 190, 109356. https://doi.org/10.1016/j.mssp.2025.109356.

[17] Ouabane M., Alaqarbeh M., Hajji H., Tabti K., Ajana M. A., Sbai A., Sekkate C., Lakhlifi T., and Bouachrine M. (**2024**) Quality Control of Coumarins, Furocoumarins and Polymethoxyflavones in Citrus Essential Oils: In Silico Analysis. ChemistrySelect, 9, e202303037. https://doi.org/10.1002/slct.202303037.

[18] Ouabane M., Zaki K., Zaki H., Guendouzi A., Sbai A., Sekkate C., Lakhlifi T., and Bouachrine M. (**2024**) Inhibition of the Janus kinase protein (JAK1) by the A. Pyrethrum Root Extract for the treatment of Vitiligo pathology: Design, Molecular Docking, ADME-Tox, MD Simulation, and in-silico investigation. Comput. Biol. Med., 179, 108816. https://doi.org/10.1016/j.compbiomed.2024.108816.

[19] Azaid A., Abram T., Kacimi R., Raftani M., Sbai A., Lakhlifi T., and Bouachrine M. (**2022**) The photophysical properties and electronic structures of ((2E,2'E)-1,1'-[chalcogen bis(4,1-phenylene)] bis [3-(4-chlorophenyl) prop-2-en-1-one] derivatives as hole-transporting materials for organic light-emitting diodes (OLEDs): Quantum chemical investigations. Mor. J. Chem., 10, 830–850. https://doi.org/10.48317/IMIST.PRSM/morjchem-v10i4.34457.

[20] Surya S. G., Raval H. N., Ahmad R., Sonar P., Salama K. N., and Rao V. R. (**2019**) Organic field effect transistors (OFETs) in environmental sensing and health monitoring: A review. TrAC - Trends Anal. Chem., 111, 27–36. https://doi.org/10.1016/j.trac.2018.11.027.

[21] Murad A. R., Iraqi A., Aziz S. B., Abdullah S. N., and Brza M. A. (**2020**) Conducting polymers for optoelectronic devices and organic solar cells: A review. Polymers (Basel), 12, 2627. https://doi.org/10.3390/polym12112627.

[22] Scholz S., Kondakov D., Lüssem B., and Leo K. (**2015**) Degradation mechanisms and reactions in organic light-emitting devices. Chem. Rev., 115, 8449–8503. https://doi.org/10.1021/cr400704v.

[23] Jeux V., Segut O., Demeter D., Rousseau T., Allain M., Dalinot C., Sanguinet L., Leriche P., and Roncali J. (**2015**) One step synthesis of DAD chromophores as active materials for organic solar cells by basic condensation. Dyes Pigm., 113, 402–408. https://doi.org/10.1016/j.dyepig.2014.09.012.

[24] Chen W. C., Yuan Y., Wu G. F., Wei H. X., Ye J., Chen M., Lu F., Tong Q.-X., Wong F. L., and Lee C. S. (**2015**) Molecular modification on bisphenanthroimidazole derivative for deep-blue organic electroluminescent material with ambipolar property and high performance. Org. Electron., 17, 159–166. https://doi.org/10.1016/j.orgel.2014.11.024.

[25] Jin R. F. and Chang Y. F. (**2015**) A theoretical study on photophysical properties of triphenylamine-cored molecules with naphthalimide arms and different π-conjugated bridges as organic solar cell materials. Phys. Chem. Chem. Phys., 17, 2094–2103. https://doi.org/10.1039/C4CP04394D.

[26] Batenko N. and Gaile A. (**2025**) 2-Substituted benzothiazole-based sensors for optical detection of biogenic amines and ammonia (microreview). Chem. Heterocycl. Compd., 1–3. https://doi.org/10.1007/s10593-025-03396-6.

[27] Klenina O. V., Chaban T. I., Chaban I. H., and Lelyukh M. I. (**2025**) Recent advances in the synthesis of thiazolo[4,5-b]pyridines. Part 3. Focus on biological activity (microreview). Chem. Heterocycl. Compd., 1–4. https://doi.org/10.1007/s10593-025-03398-4.

[28] Azazi A., Mabrouk A., Chemek M., Kreher D., and Alimi K. (**2014**) DFT modeling of conjugated copolymers photophysical properties: towards organic solar cell application. Synth. Met., 198, 314–322. https://doi.org/10.1016/j.synthmet.2014.10.015.

[29] Wu Y. and Zhu W. (**2013**) Organic sensitizers from D–p–A to D–A–p–A: effect of the internal electron-withdrawing units on molecular absorption, energy levels and photovoltaic performances. Chem. Soc. Rev., 42, 2039–2058. https://doi.org/10.1039/C2CS35346F.

[30] Brütting W. (**2005**) Introduction to the Physics of Organic Semiconductors. Phys. Org. Semicond., 1–14. https://doi.org/10.1002/3527606637.ch.

[31] Özen A. S., Atilgan C., and Sonmez G. (**2007**) Noncovalent intramolecular interactions in the monomers and oligomers of the acceptor and donor type of low band gap conducting polymers. J. Phys. Chem. C, 111, 16362–16371. https://doi.org/10.1021/jp074380n.

[32] Cheminet N., Nogueira S. L., Benaqqa O., El Malki Z., Bourass M., Cassegrain S., Hamidi M., Bouachrine M., Sotiropoulos J. M., Miqueu K., Jarrosson T., Niebel C., Lère-Porte J. P., and Serein-Spirau F. (**2020**) Elaboration of low-band-gap π-conjugated systems based on thieno[3,4-b]pyrazines. Pure Appl. Chem., 92, 335–353. https://doi.org/10.1515/pac-2018-1009.

[33] Zangoli M., Monti F., Zanelli A., Marinelli M., Flammini S., Spallacci N., and Di Maria F. (**2024**) Multifunctional photoelectroactive materials for optoelectronic applications based on thieno[3,4-b]pyrazines and thieno[1,2,5]thiadiazoles. Chem. Eur. J., 30(7), e202303590. https://doi.org/10.1002/chem.202303590.

[34] Gómez-Jiménez M. D., Pou-Amrigo R., and Ortí E. (**2009**) A theoretical study of the low-lying excited states of thieno[3,4-b]pyrazine. J. Chem. Phys., 131, 244303. https://doi.org/10.1063/1.3274816.

[35] Chen L. Q., Chen L. D., Kalinin S. V., Klimeck G., Kumar S. K., Neugebauer J., and Terasaki I. (**2015**) Design and discovery of materials guided by theory and computation. NPJ Comput. Mater., 1(1), 1–2. https://doi.org/10.1038/npjcompumats.2015.1.

[36] Cavasotto C. N., Aucar M. G., and Adler N. S. (**2019**) Computational chemistry in drug lead discovery and design. Int. J. Quantum Chem., 119(2), e25678. https://doi.org/10.1002/qua.25678.

[37] Russo T. V., Martin R. L., and Hay P. J. (**1994**) Density Functional Calculations on First-Row Transition Metals. J. Chem. Phys., 101, 7729–7737. https://doi.org/10.1063/1.468265.

[38] Srivastava R., Al-Omary F. A. M., El-Emam A. A., Pathak S. K., Karabacak M., Narayan V., Chand S., Prasad O., and Sinha L. (**2017**) A combined experimental and theoretical DFT (B3LYP, CAM-B3LYP and M06-2X) study on electronic structure, hydrogen bonding, solvent effects and spectral features of methyl 1H-indol-5-carboxylate. J. Mol. Struct., 1137, 725–741. https://doi.org/10.1016/j.molstruc.2017.02.084.

[39] Irfan A. and Mahmood A. (**2018**) Designing of efficient acceptors for organic solar cells: molecular modelling at DFT level. J. Clust. Sci., 29(2), 359–365. https://doi.org/10.1007/s10876-018-1338-x

[40] Franco Jr F. C. and Padama A. A. B. (**2016**) DFT and TD-DFT study on the structural and optoelectronic characteristics of chemically modified donor–acceptor conjugated oligomers for organic polymer solar cells. Polymer, 97, 55–62. https://doi.org/10.1016/j.polymer.2016.05.025.

[41] Dkhissi A., Ouhib F., Chaalane A., Hiorns R. C., Dagron-Lartigau C., Iratcabal P., and Pouchan C. (**2012**) Theoretical and experimental study of low band gap polymers for organic solar cells. Phys. Chem. Chem. Phys., 14(16), 5613–5619. https://doi.org/10.1039/C2CP40170C.

[42] Johansson T., Mammo W., Svensson M., Andersson M. R., and Inganäs O. (**2003**) Electrochemical bandgaps of substituted polythiophenes. J. Mater. Chem., 13(6), 1316–1323. https://doi.org/10.1039/B301403G.

[43] Nasab E. A., Nasseh N., Damavandi S., Amarzadeh M., Ghahrchi M., Hoseinkhani A., and Danaee I. (**2023**) Efficient purification of aqueous solutions contaminated with sulfadiazine by coupling electro-Fenton/ultrasound process: optimization, DFT calculation, and innovative study of human health risk assessment. Environ. Sci. Pollut. Res., 30(35), 84200–84218. https://doi.org/10.1007/s11356-023-28235-z.

[44] Tirado-Rives J. and Jorgensen W. L. (**2008**) Performance of B3LYP density functional methods for a large set of organic molecules. J. Chem. Theory Comput., 4(2), 297–306. https://doi.org/10.1021/ct700248k.

[45] Zaki K., Ouabane M., Sbai A., Sekkate C., Lakhlifi T., and Bouachrine M. (**2025**) Unraveling the mechanism, regioselectivity, and stereoselectivity of [3 + 2] cycloaddition reactions for anticancer spirooxindole derivatives: A density functional theory study. Comput. Theor. Chem., 1245, 115086. https://doi.org/10.1016/j.comptc.2025.115086.

[46] Azaid A., Raftani M., Alaqarbeh M., Kacimi R., Abram T., Khaddam Y., Nebbach D., Sbai A., Lakhlifi T., and Bouachrine M. (**2022**) New organic dye-sensitized solar cells based on the D-A-π-A structure for efficient DSSCs: DFT/TD-DFT investigations. RSC Adv., 12, 30626–30638. https://doi.org/10.1039/d2ra05297k.

[47] Armon A. M., Bedi A., Borin V., Schapiro I., and Gidron O. (**2021**) Bending versus twisting acenes – a computational study. Eur. J. Org. Chem., 2021(39), 5424–5429. https://doi.org/10.1002/ejoc.202100865 .

[48] Narsaria A. K., Poater J., Fonseca Guerra C., Ehlers A. W., Hamlin T. A., Lammertsma K., and Bickelhaupt F. M. (**2020**) Distortion-controlled redshift of organic dye molecules. Chem. Eur. J., 26(9), 2080–2093. https://doi.org/10.1002/chem.201905355.

[49] Raftani M., Abram T., Azaid A., Kacimi R., Bennani M. N., and Bouachrine M. (**2021**) Theoretical design of new organic compounds based on diketopyrrolopyrrole and phenyl for organic bulk heterojunction solar cell applications: DFT and TD-DFT study. Mater. Today: Proc., 45, 7334–7343. https://doi.org/10.1016/j.matpr.2020.12.1228.

[50] Kacimi R., Raftani M., Abram T., Azaid A., Ziyat H., Bejjit L., Bennani M. N., and Bouachrine M. (**2021**) Theoretical design of D-π-A system new dyes candidate for DSSC application. Heliyon, 7, e07171. https://doi.org/10.1016/j.heliyon.2021.e07171.

[51] Kacimi R., Ali U., Azaid A., Sarfaraz S., Raftani M., Bejjit L., and Bouachrine M. (**2024**) Quantum chemical study of symmetrical non-fullerene acceptor chromophores for organic photovoltaics. Comput. Theor. Chem., 1233, 114475. https://doi.org/10.1016/j.comptc.2024.114475.

[52] Kacimi R., Hayn R., Makhfudz I., Azaid A., Bejjit L., and Bouachrine M. (**2025**) Designing small push-pull chromophores hole transport materials for perovskite solar cells (PSCs) and organic solar cells with optimum performance. J. Photochem. Photobiol. A: Chem., 464, 116315. https://doi.org/10.1016/j.jphotochem.2025.116315.

[53] Rocha M., Di Santo A., Arias J. M., Gil D. M., and Ben Altabef A. (**2015**) Ab-initio and DFT calculations on molecular structure, NBO, HOMO-LUMO study and a new vibrational analysis of 4-(Dimethylamino)benzaldehyde. Spectrochim. Acta A Mol. Biomol. Spectrosc., 136, 635–643. https://doi.org/10.1016/j.saa.2014.09.077.

[54] Choudhary V. K., Bhatt A. K., Dash D., and Sharma N. (**2019**) DFT calculations on molecular structures, HOMO–LUMO study, reactivity descriptors and spectral analyses of newly synthesized diorganotin(IV) 2-chloridophenylacetohydroxamate complexes. J. Comput. Chem., 40, 2354–2363. https://doi.org/10.1002/jcc.26012.

[55] Bourass M., Touimi Benjelloun A., Benzakour M., Mcharfi M., Jhilal F., Serein-Spirau F., Sotiropoulos J. M., and Bouachrine M. (**2017**) DFT/TD-DFT characterization of conjugational electronic structures and spectral properties

of materials based on thieno[3,2-b][1]benzothiophene for organic photovoltaic and solar cell applications. J. Saudi Chem. Soc., 21, 563–574. https://doi.org/10.1016/j.jscs.2017.01.001.

[56] Mohan B., Jana A., Das N., Bharti S., Choudhary M., Muhammad S., Kumar S., Al-Sehemi A. G., and Algarni H. (**2019**) A dual approach to study the key features of nickel(II) and copper(II) coordination complexes: synthesis, crystal structure, optical and nonlinear properties. Inorg. Chim. Acta, 484, 148–159. https://doi.org/10.1016/j.ica.2018.09.037.

[57] Bibi S., Shafiq-ur-Rehman, Jia R., Zhang H. X., and Bai F. Q. (**2019**) Effect of different topological structures (D-π-D and D-π-A-π-D) on the optoelectronic properties of benzo[2,1-b:3,4-b′]dithiophene based donor molecules toward organic solar cells. Sol. Energy, 186, 311–322. https://doi.org/10.1016/j.solener.2019.04.043.

[58] Shafiq I., Shoukat U., Adnan Asghar M., Aslam M., Ahamad T., Ahmed S., Bullo S., and Chandra Ojha S. (**2024**) Structural tailoring via end-capped acceptors of thiophene-based C-shaped non-fullerene compounds with A-π-A backbone for the exploration of photovoltaic response. J. Saudi Chem. Soc., 28, 101799. https://doi.org/10.1016/j.jscs.2023.101799.

[59] Etabti H., Fitri A., Touimi Benjelloun A., Benzakour M., and Mcharfi M. (**2022**) Efficient tuning of benzocarbazole based small donor molecules with D-π-A-π-D configuration for high-efficiency solar cells via π-bridge manipulation: a DFT/TD-DFT study. Comput. Theor. Chem., 1208, 113580. https://doi.org/10.1016/j.comptc.2021.113580.

[60] Khan M. U., Anwar A., Hassan A. U., Alshehri S. M., and Sohail A. (**2024**) DFT simulations of photovoltaic parameters of dye-sensitized solar cells with new efficient sensitizer of indolo[3,2-b]carbazole complexes. Energies Sci. Eng., 12(9), 3681–3703. https://doi.org/10.1002/ese3.1834.

[61] Pan Y., Liu X., Zhang W., Liu Z., Zeng G., Shao B., Liang Q., He Q., Yuan X., Huang D., and Chen M. (**2020**) Advances in photocatalysis based on fullerene C60 and its derivatives: properties, mechanism, synthesis, and applications. Appl. Catal. B, 265, 118579. https://doi.org/10.1016/j.apcatb.2019.118579.

[62] Setsoafia D. D. Y., Ram K. S., Mehdizadeh-Rad H., Ompong D., Murthy V., and Singh J. (**2022**) DFT and TD-DFT calculations of orbital energies and photovoltaic properties of small molecule donor and acceptor materials used in organic solar cells. J. Renew. Mater., 10, 2553–2567. https://doi.org/10.32604/jrm.2022.020967.

[63] Mehboob M. Y., Khan M. U., Hussain R., Ayub K., Sattar A., Ahmad M. K., Irshad Z., Saira S., and Adnan M. (**2021**) Designing of benzodithiophene core-based small molecular acceptors for efficient non-fullerene organic solar cells. Spectrochim. Acta A Mol. Biomol. Spectrosc., 244, 118873. https://doi.org/10.1016/j.saa.2020.118873.

[64] Nebbach D., Agda F., Lakhlifi T., Ajana M. A., Kaya S., Siddique F., Lgaz H., and Bouachrine M. (**2022**) Designing new donors organic compounds with IDIC core for photovoltaic application. Optik (Stuttg.), 262, 169174. https://doi.org/10.1016/j.ijleo.2022.169174.

[65] Mehboob M. Y., Hussain R., Adnan M., Saira S., Farwa U., Irshad Z., and Saeed Ashraf Janjua M. R. (**2022**) Theoretical modelling of novel indandione-based donor molecules for organic solar cell applications. J. Phys. Chem. Solids, 162, 110508. https://doi.org/10.1016/j.jpcs.2021.110508.

[66] Azaid A., Abram T., Alaqarbeh M., Raftani M., Kacimi R., Sbai A., Lakhlifi T., and Bouachrine M. (**2023**) Design new organic material based on triphenylamine (TPA) with D-π-A-π-D structure used as an electron donor for organic solar cells: a DFT approach. J. Mol. Graph. Model., 122, 108470. https://doi.org/10.1016/j.jmgm.2023.108470.

[67] Khalid M., Ali A., Jawaria R., Asghar M. A., Asim S., Khan M. U., Hussain R., Fayyaz ur Rehman M., Ennis C. J., and Akram M. S. (**2020**) First principles study of electronic and nonlinear optical properties of A-D-π-A and D-A-D-π-A configured compounds containing novel quinoline-carbazole derivatives. RSC Adv., 10, 22273–22283. https://doi.org/10.1039/d0ra02857f.

[68] Azaid A., Alaqarbeh M., Abram T., Raftani M., Kacimi R., Khaddam Y., Sbai A., Lakhlifi T., and Bouachrine M. (**2024**) D-π-A push-pull chromophores based on N,N-Diethylaniline as a donor for NLO applications: effects of structural modification of π-linkers. J. Mol. Struct., 1295, 136602. https://doi.org/10.1016/j.molstruc.2023.136602.

[69] Bouachrine M., Azaid A., Abram T., Kacimi R., Raftani M., Sbai A., and Lakhlifi T. (**2021**) DFT/TDDFT studies of the structural, electronic, NBO and non-linear optical properties of triphenylamine functionalized tetrathiafulvalene. Turk. Comput. Theor. Chem., 5, 24–34. https://doi.org/10.33435/tcandtc.926405.

[70] Karabacak M., and Yilan E. (**2012**) Molecular structure, spectroscopic (FT-IR, FT-Raman, 13C and 1H NMR, UV), polarizability and first-order hyperpolarizability, HOMO and LUMO analysis of 4′-methylbiphenyl-2-carbonitrile. Spectrochim. Acta A Mol. Biomol. Spectrosc., 87, 273–285. https://doi.org/10.1016/j.saa.2011.11.051.

[71] Jawaria R., Hussain M., Khalid M., Shahid M., Hameed A., Khan I. U., and Ghaffar A. (**2019**) Synthesis, crystal structure analysis, spectral characterization and nonlinear optical exploration of potent thiosemicarbazones based compounds: A DFT refine experimental study. Inorg. Chim. Acta, 486, 162–171. https://doi.org/10.1016/j.ica.2018.10.035.

[72] Khalid M., Ali A., Jawaria R., Asghar M. A., Asim S., Khan M. U., and Akram M. S. (**2020**) First principles study of electronic and nonlinear optical properties of A–D–π–A and D–A–D–π–A configured compounds containing novel quinoline–carbazole derivatives. RSC Adv., 10(37), 22273–22283. https://doi.org/10.1039/D0RA02857F.

© 2026 by the authors; licensee Growing Science, Canada. This is an open access article distributed under the terms and conditions of the Creative Commons Attribution (CC-BY) license (http://creativecommons.org/licenses/by/4.0/).